Investigation of Ice-PVC separation under Flexural Loading using FEM Analysis

H. Xue*, H. Khawaja
Faculty of Engineering and Technology, UiT The Arctic University of Norway, Norway

ABSTRACT
This paper presents the FEM technique applied in the study of ice separation over a polyvinyl chloride (PVC) surface. A two layer model of ice and PVC is analysed theoretically using Euler-Bernoulli beam theory and the rule of mixtures. The physical samples are prepared by freezing ice over the PVC surfaces. The samples are tested experimentally in a four-point loading setup. The experimental results contain strain data gathered through a data acquisition system using the LabView® software. The data is collected at the rate of 1 kHz per load step. A model is also coded in MATLAB® and simulated using the finite element method (FEM) in ANSYS® Multiphysics. The FEM model of the ice and PVC sample is built using solid elements. The mesh is tested for sensitively. A good agreement is found between the theoretical, experimental and numerical simulation results.

1. INTRODUCTION

The phenomenon of icing is referred to when water droplets are cooled below the freezing temperature (0°C) and freeze upon impact with a structure [1]. Ice exists in a number of different crystal structures, as well as two amorphous states [2]. The ordinary ice we find in our freezer is hexagonal crystal structure that is called ice – 1 h, where the numbers refer to individual water molecules [3]. The physical properties and the appearance of accreted ice varies widely [4, 5]. It is known from published work that Young's modulus of ice varies between 4 GPa to 9 GPa [6-8]. In addition, it has also been reported that value of Young's modulus for ice is related to temperature, grain size, density and sample volume.

Icing causes many serious problems, for example, icing causes aircraft accidents [9, 10], icing on ship hulls creates navigational problems [9] and icing on wind turbines has many negative consequences [11, 12]. These challenges are associated with the ice adhesive behaviour [13].

There is no direct correlation to calculate the ice adhesion force [14]. However, researchers have given number of theories [15, 16]. The theories divide the force of adhesion into four categories: electrostatic adhesion [17, 18], diffusive adhesion [19, 20], mechanical adhesion, and chemical adhesion [21].

The most common reason of ice adhesion is mechanical. The ice adheres when water seeps into the microscopic pores of the material substrate and freezes, thereby, forming an interlocking mechanism [22]. Therefore, surface roughness has a significant effect on ice adhesion. For example, ice adhesion on the surface of un-polished stainless steel, in general,

*Corresponding Author: hxu001@uit.no

is up to 1.65 MPa, while the ice adhesion on polished stainless steel is only 0.07 MPa [14].

In the given study, ice is frozen over a PVC surface. PVC is a polymer-based structure, and its mechanical properties may vary based on curing process [23]. In addition, additives can be added to obtain a range of mechanical properties, for example [24] studied mechanical properties of PVC with the addition of polyethylene oxide. In this study, soft and pure PVC is used. It is reported that its Young's modulus can vary in the range of 1.5 MPa to 15 MPa [23]. An experiment based study reported by [24] found the Young's modulus of PVC to be around 7 MPa.

2. METHODOLOGY

In order to approach to the problem of the adhesion of ice, a two layer laminate structure of ice and polymer material is designed. A four-point bending test is applied to investigate the separation of ice from a PVC surface. Different methods are used to analyse the results: theoretical, experimental and numerical simulations.

For the theoretical analysis the Euler-Bernoulli beam theory [25] is solved in MATLAB®. For experimental work, ice is frozen over the PVC surface and loaded in a four-point bending test bench with a mounted strain gauge. The numerical study is performed in ANSYS® Multiphysics by modelling the two materials: ice and PVC. The results from these studies reveal the longitudinal and shear stresses at the interface of the PVC surface and the ice separation behaviour.

2.1 Theoretical Analysis

The Euler-Bernoulli beam theory [25] can be used to calculate the maximum deflection in the centre of the four-point bending specimen. Maximum deflection δ_{max} is given in Equation (1):

$$\delta_{max} = \delta_{center} = \frac{PL_1}{48EI_t}(3L^2 - 4L_1^2) \tag{1}$$

where δ_{center} is the deflection in the centre, L is the total length, L_1 is the distance between support point to loading point, E is Young's modulus and I is total moment of inertia about the neutral axis.

This specimen contains ice and PVC, two kinds of different materials, and therefore the rule of mixtures is introduced to find the material properties of the sample. It is valid to assume that under tensile loading, the Young's moduli of the sample can be described as given in Equation (2):

$$E = E_{ice}\frac{A_{ice}}{A} + E_p\frac{A_p}{A} \tag{2}$$

where E, E_{ice} and $E_p$are Young's moduli of the sample, ice and PVC respectively. A, A_{ice} and $A_p$are cross-sectional areas of the sample, ice and PVC respectively.

Stress calculations in beams are performed with respect to the neutral axis. The neutral axis of a beam goes through the centroid of its cross section. Since there are two materials that have

different young's moduli E_{ice} and E_p, it is safe to assume that $E_{ice} > E_p$, the expansion factor, also known as balance coefficient (n), is given in Equation (3):

$$n = \frac{E_p}{E_{ice}} \tag{3}$$

In order to have a similar inertial effect of both materials, the balance coefficient is multiplied by the width of PVC to create a hypothetical area. The neutral axis of the sample shifts because of the difference in the Young's moduli of ice and PVC, similarly, the values of the moment of area and the moment of Inertia also change. These values are required to be calculated with respect to the new neutral axis (Equation (3)). The total moment of area Q_t and inertia I_t are given in Equations (4) and (5):

$$Q_t = Q_{ice} + Q_p \tag{4}$$

$$I_t = I_{ice} + I_p \tag{5}$$

where Q_{ice} is the area moment of ice, Q_p is area moment of PVC, I_{ice} is the moment of inertia of ice and I_p is the moment of inertia of PVC. Q_{ice} , Q_p , I_{ice} and I_p are given in Equations (6) to (9):

$$Q_{ice} = t_{ice} \cdot b \cdot (\overline{y}_{ice} - \overline{Y}) \tag{6}$$

$$Q_p = t_p \cdot n \cdot b \cdot (\overline{y}_p - \overline{Y}) \tag{7}$$

$$I_{ice} = \frac{b \cdot t_{ice}^3}{12} + b \cdot t_{ice} \cdot (\overline{y}_{ice} - \overline{Y})^2 \tag{8}$$

$$I_p = \frac{n \cdot b \cdot t_p^3}{12} + n \cdot b \cdot t_p \cdot (\overline{y}_p - \overline{Y})^2 \tag{9}$$

where $\overline{y}_{ice}$ and $\overline{y}_p$ are distances of the neutral axis of ice and PVC from the reference axis respectively.

The longitudinal stresses in the ice and PVC are given in Equations (10) and (11):

$$\sigma_{x,ice} = -\frac{M\left(y - \overline{Y}\right)}{I_t}, \qquad (t_p \le y \le t_p + t_{ice}) \tag{10}$$

$$\sigma_{x,p} = -\frac{nM\left(y - \overline{Y}\right)}{I_t}, \qquad (0 \le y \le t_p) \tag{11}$$

where $\sigma_{x,ice}$ and $\sigma_{x,p}$ are the longitudinal stresses in ice and PVC respectively. y is the position based on reference axis (placed at the bottom of the sample).

Similarly, shear stresses in the ice and PVC are given in Equations (12) and (13):

$$\tau_{x,ice} = \frac{VQ_{ice}}{I_t\, b}, \qquad (y = t_p) \tag{12}$$

$$\tau_{x,p} = \frac{nVQ_p}{I_t\, b}, \qquad (y = t_p) \tag{13}$$

where $\tau_{x,ice}$ and $\tau_{x,p}$ are the shear stresses at the interface of ice and PVC respectively.

2.2 Experimental Setup

The aim of the experiment is to generate observations of ice separation on a laboratory scale since bending induces longitudinal and shear stresses. Samples are prepared by freezing ice from tap water over the PVC surfaces (on the opposite side to the location of strain gauge) at -10℃ over 12 hours in the cold room test facility at UiT-The Arctic University of Norway (Narvik Campus). The length of the PVC plate is 260 mm and all of this is covered with ice. The width and the thickness of the plate are 60mm and 1mm, respectively. The experiments are performed in the same conditions in order to avoid building any cracks in sample due to thermal shock. Thermal shock may introduce cracks in the ice samples and hence lead to erroneous results [26].

In order to investigate the separation of ice from a PVC surface, a four-point bending test bench is set up. Two different samples with ice thickness of 3 mm and 5 mm are investigated. In this setup the distance between the two supporting points is 200mm and the distance from the supporting point to the loading point is 20mm as shown in Figure 1.

In these experiments, loads are in the form of weights. These weights are placed gently by hand to produce strain in the sample. Strains are recorded using a rosette strain gauge adhered to the bottom of a PVC sample as shown in Figure 2. The strain gauge is attached to a Wheatstone bridge circuit to give variation in voltage with the change in resistance. In this study, TML® FRA-5-23 strain gauges are used. These strain gauges have a gauge factor value of 2.15. The voltages are recorded using a data acquisition system. In this study a National Instrument® USB-6351 model, X Series Data Acquisition device is used to record strain. To connect the instrumental circuitry, various other cables, accessories, along with the data

acquisition device are connected to a computer. The data is recorded in the National Instrument LabView® program. The data is recorded at 1 kHz over 1 sec for each load. It allows measuring of the strain more accurately since data can be averaged over time. Crude data (.lvm files) are processed in MS Excel to calibrate the results. The parameters are shown in Table 1.

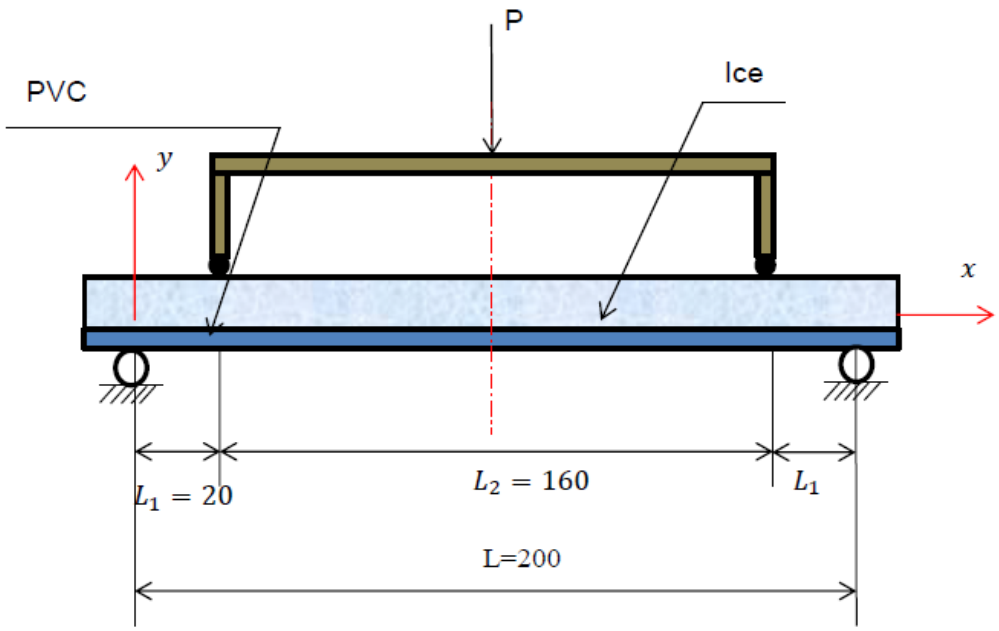

Figure 1: Four-point bending test setup of ice and PVC

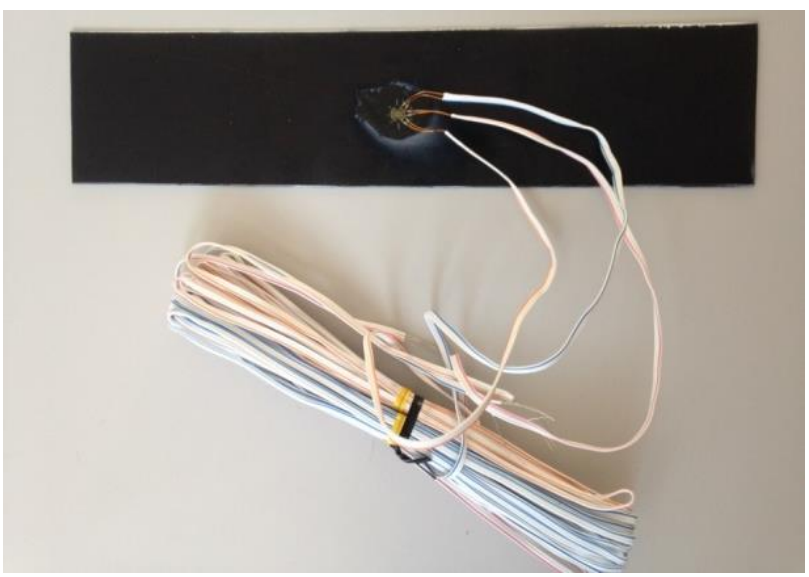

Figure 2: PVC surface of 260 X 60 X 1 mm with a rosette strain gauge mounted in its geometric centre.

Table 1: Description and values of parameters

Description	Variable	Units	value
Length of PVC and ice sample	l	mm	260
Width of PVC and ice sample	b	mm	60
Thickness of PVC	t_p	mm	1
Thickness of ice for sample 1	t_{ice}	mm	3
Thickness of ice for sample 2	t_{ice}	mm	5
Distance between the support and the load points	L_1	mm	20
Distance between the two load points	L_2	mm	160
Distance between the two support points	L	mm	200
Loads	P	g	varied

2.3 Numerical Simulations

The numerical studies are performed in ANSYS® Multiphysics. The geometric model is built in the ANSYS® Multiphysics structural module. The dimensions of the geometric model are 260 mm long and 60 mm wide. The geometric model contains 12 volume segments. The volume segments provide the geometric features required to place the loading and boundary conditions on the model. The finite element (FE) model of ice and PVC sample is built using ANSYS® finite element (FE) brick 20 nodes solid 186 elements [27] using linear elastic isotropic material model. This element type provides more accurate results in comparison to solid 8 node brick 185 elements. However, the simulation run-time for solid 186 is considerably higher than solid 185 elements.

The FE models are tested for sensitivity by varying the element numbers as shown in Figure 3. Net displacement results for a node at a particular geometric location are used to test the sensitivity. Result for an FEM mesh of 31200 elements is considered as a reference. For other meshes, variations are calculated as given in Equation (14).

$$Fractional\ displacement\ results\ = \frac{Displacement_{Number\ of\ Elements}}{Displacement_{31200\ Elements}} \tag{14}$$

As shown in Figure 3 that FEM results are consistent with a number of elements equal to 7240, therefore it is valid to use an FEM model containing 10800 elements for further analysis. The displacement constraint is applied at the point of supports as shown in Figure 4. In FEM, the displacement constraints are applied in x and y directions. It is to be noted that the longitudinal axis is oriented in the z direction in this model. The forces are applied equally to the nodes as shown in Figure 5.

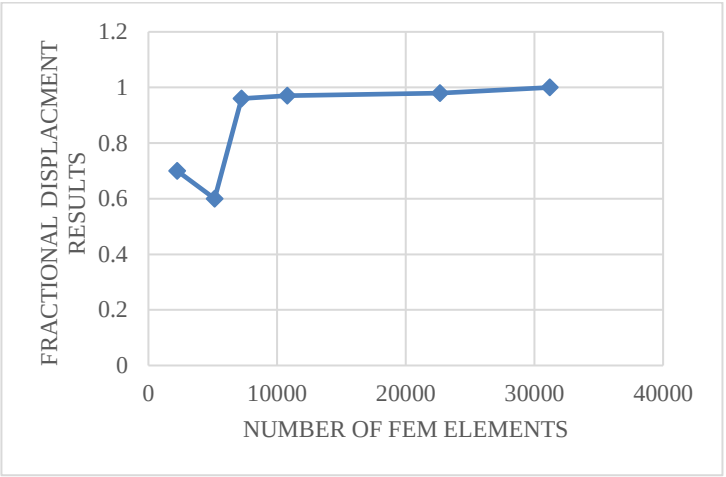

Figure 3: FEM meshes sensitivity analysis.

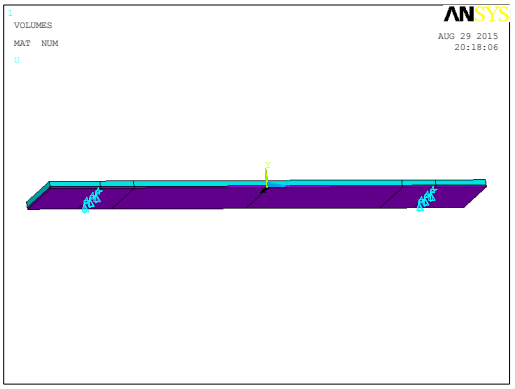

Figure 4: Applied displacements constraints on FEM model.

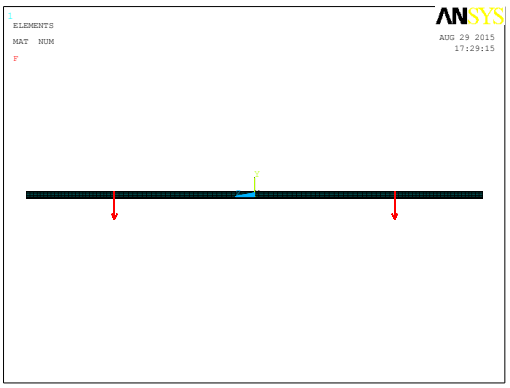

Figure 5: Applied forces on FEM model.

3. RESULTS AND DISCUSSION

The results are given in three sections; theoretical, experimental and numerical simulation results. Theoretical results are obtained by solving Euler-Bernoulli beam theory for four-point bending in MATLAB®. Experimental results are achieved via strain gauge in four-point bending test bench. And numerical results are from linear static analysis in ANSYS® Multiphysics.

3.1 Theoretical Results

Three different results were obtained through theoretical analysis, i.e. maximum displacements in the samples with load, stress profile with a thickness of the sample beam, stress profile in the longitudinal direction of the sample beam.

The maximum displacement in the samples is calculated using the correlation of Equation (1) which is based on beam theory. To find the limits of theoretical results, the variation in gradient $\left(\frac{\delta_{max}}{P}\right)$ is tabulated as given in Table 2. It is shown that gradient values are more sensitive to the Young's modulus of ice in comparison to the Young's modulus of PVC.

Table 2: Gradient of maximum displacements with loads with variations in Young's moduli of ice and PVC

t_{ice} (mm)	Gradient ($\frac{mm}{g}$) E_{ice} = 4 GPa E_p = 1.5 MPa	Gradient ($\frac{mm}{g}$) E_{ice} = 9 GPa E_p = 1.5 MPa	Gradient ($\frac{mm}{g}$) E_{ice} = 4 GPa E_p = 15 MPa	Gradient ($\frac{mm}{g}$) E_{ice} = 9 GPa E_p = 15 MPa
3 mm	0.0012	5.31E-04	0.0012	5.29E-04
5 mm	2.32E-04	1.03E-04	2.31E-04	1.03E-04

The maximum displacements with loads for an ice Young's modulus of 4 GPa and a PVC Young's modulus of 15 MPa for a 5 mm thick ice sample are shown in Figure 6, which is produced using MATLAB® script.

The longitudinal stress is independent of the material property such as Young's modulus and directly proportional to the applied load. The maximum stress in the sample is limited by tensile strength. Stress more than the tensile strength will cause ice to fracture. The tensile strength of ice has been reported to be between 1 MPa to 1.5 MPa [28]. Loads responsible for this amount of stresses are given below: Maximum Longitudinal Stress across the thickness of a 3 mm ice sample under a load of 1000-1400 is 1.080-1.512MPa; Maximum Longitudinal Stress across the thickness of a 5 mm ice sample under a load of 2600-3900g is 1.016-1.523MPa. Figure 7 is shown the longitudinal stress across the thickness of a 5 mm ice sample under a load of 3900g.

As shown, the tensile stress is maximum at the interface between ice and PVC and compressive stress is maximum at the top of the ice. There is negligible stress in PVC since it is softer than ice. The negative value of longitudinal stresses corresponds to compressive stresses. The longitudinal stress across the length of the sample for a 5 mm ice sample under a load of 3900 g is shown in Figure 8. It is shown that longitudinal stress is zero beyond the support point and varying linearly between the supports and loading points.

The shear stress is a function of material properties such as Young's modulus. The shear stress values of the samples are shown with the Young's moduli of ice and PVC in Table 3. The shear stress causes the ice to separate from PVC. The adhesive strength of ice on a PVC

surface is reported to be 234421 Pa (~34 psi) [22]. It is found that the shear stress experienced by the samples under maximum tensile loading is far less than this value. Therefore, it can be assumed that ice will undergo tensile failure prior to separation from a PVC surface. It is calculated that for a 3 mm thick ice sample that it will break and separate under a load of 1000-1400 g and the maximum shear stress is 270-378 Pa, for a 5 mm thick ice sample, it will break and separate under a load of 2600-3900 g and the maximum shear stress is 228-342 Pa.

Table 3: Shear stress with variations in Young's moduli of ice and PVC for a fixed load of 3500 g

t_{ice} (mm)	**Shear Stress (Pa)** E_{ice} = 4 GPa E_p = 1.5 MPa	**Shear Stress (Pa)** E_{ice} = 9 GPa E_p = 1.5 MPa	**Shear Stress (Pa)** E_{ice} = 4 GPa E_p = 15 MPa	**Shear Stress (Pa)** E_{ice} = 9 GPa E_p = 15 MPa
3 mm	95.2982	42.3737	946.1282	422.3767
5 mm	30.8891	13.7315	307.7777	137.0951

Variation in shear stress along the length of a 5 mm ice sample for an ice Young's modulus of 4 GPa and a PVC Young's modulus of 15 MPa under the load of 3900 g is given in Figure 9. It is to be noted that shear stress is zero beyond the support points and within the loading points and has a constant value between support and loading points. These results are in agreement with the four-point shear force diagram.

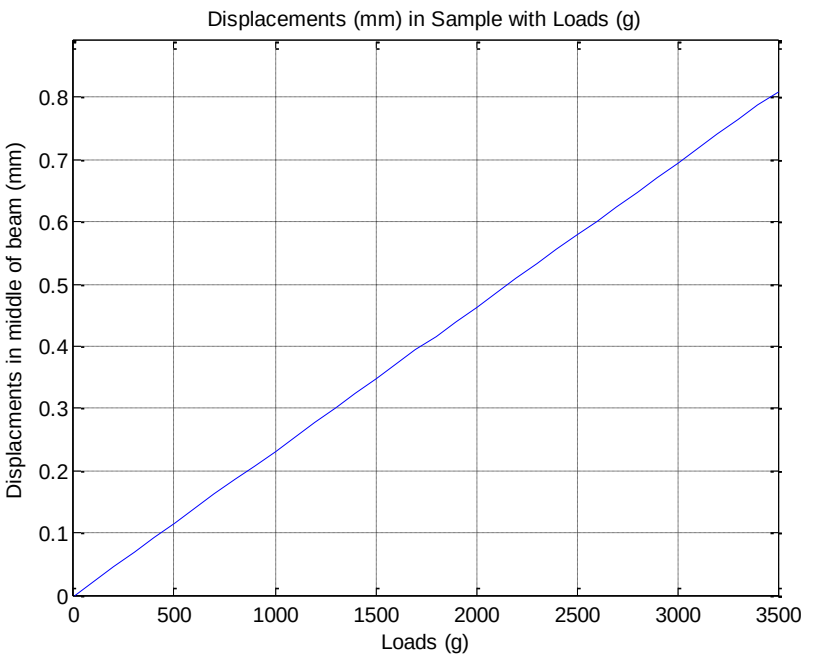

Figure 6: Displacements in middle of beam (mm) vs. loads (g) for an ice Young's modulus of 4 GPa and a PVC Young's modulus of 15 MPa for a 5 mm thick ice sample

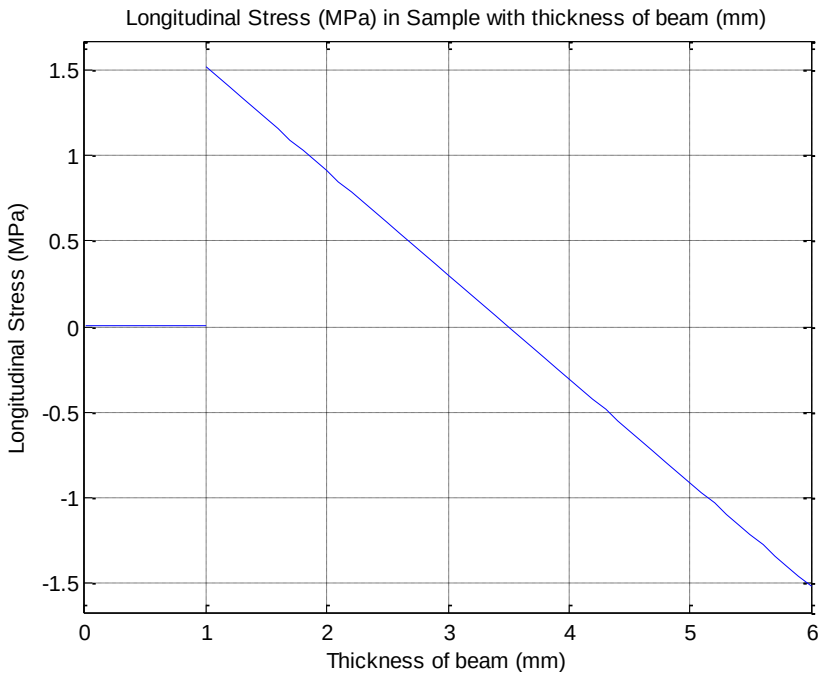

Figure 7: Longitudinal stress (MPa) along the thickness of the sample for a 5 mm ice sample under the load of 3900g.

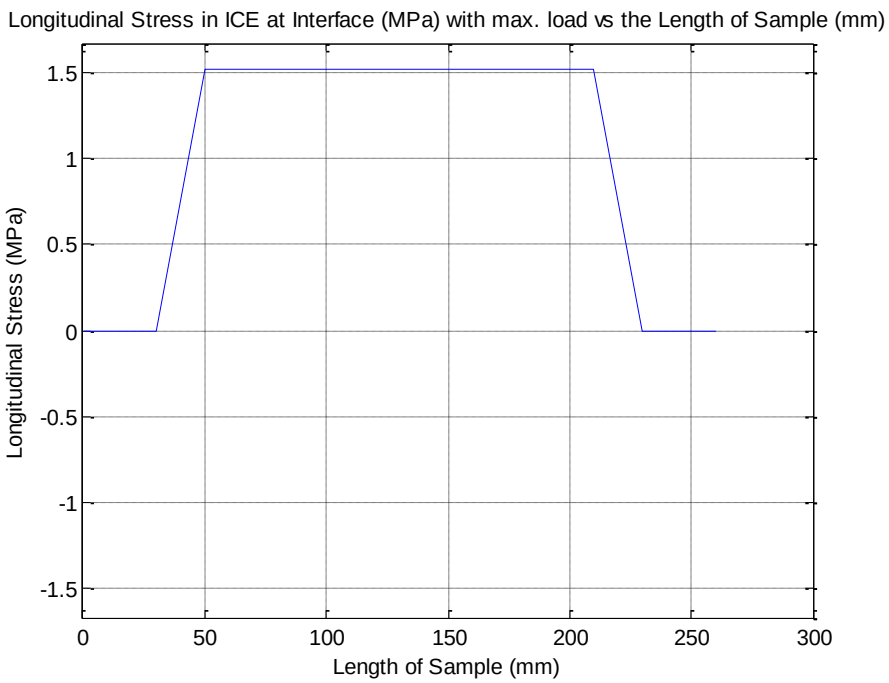

Figure 8: Longitudinal stress (MPa) along the sample length for a 5 mm ice sample under the load of 3900 g.

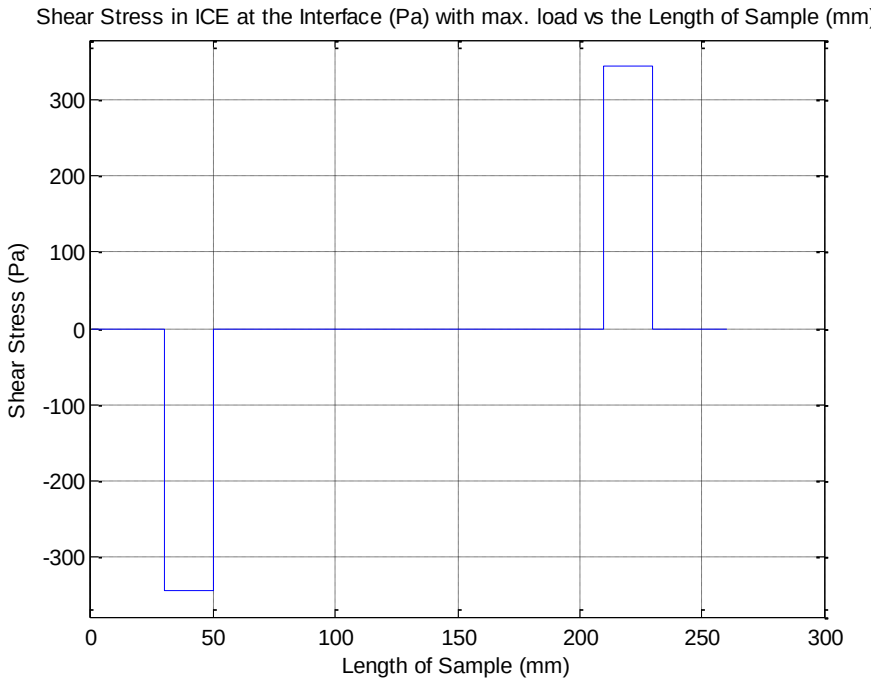

Figure 9: Variation in shear stress along the length of a 5 mm ice sample for an ice Young's modulus of 4 GPa and a PVC Young's modulus of 15 MPa under the load of 3900 g

3.2 Experimental Results

The replication of the mechanical behaviour of ice under flexural loading and the delamination of ice from the surface of PVC are the two key points to be noted. The experiments are repeated with both thicknesses 3 mm and 5 mm ice samples. The displacement with load for each sample is given in Figure 10 and Figure 11.

The experiments show that the gradient of displacement with load for 3 mm and 5 mm thickness ice samples are 1.04E-03 mm/g and 2.41E-04 mm/g, r-squared value is 80.3 % and 73.3 % respectively. R-squared values indicate the fitness of data with the proposed linear equation. These values were used to calculate the Young's Modulus of ice using the procedure given before. The results were obtained for three different Young's Modulus for PVC: 1.5 MPa, 7 MPa and 15 MPa. In addition, r-squared value indicate that experimental results of 3 mm and 5 mm samples have a deviation of 19.7% and 26.8% respectively. The experimental results for the Young's modulus of ice are given in Table 4.

It is found from the results that Young's moduli of ice do not vary with Young's moduli of PVC. Also, the obtained values of Young's modulus are in reasonable proximity to the values reported in the literature [6-8]. The deviation in the results is indicative of factors such as noise in strain gauges, handling of loads, instrumentation error, etc.

The maximum loads at the time of failure for 3mm and 5mm thickness of ice sample are 1800g and 3500g respectively. It is calculated that the corresponding longitudinal stresses for 3mm and 5mm thickness of ice sample are 1.96 MPa and 1.37 MPa respectively, and

shear stresses for each load are 41.7 Pa and 32.1Pa accordingly. It is found that maximum longitudinal stresses are in reasonable proximity of the reported values of the tensile strength of ice [28].

The failures in 3 mm and 5 mm ice samples are shown in Figure 12 and Figure 13. As shown in Figure 12: Failure in a 3 mm ice sample, that ice has gone through fractures, and a part of it is still in adhesion to the PVC surface. As shown in Figure 13, that ice has gone through fracture from various points and separated from the PVC surface. This is indicative of adhesive failure. Residuals of ice are noticeable on close observation of PVC surfaces. This is indicative of cohesive failure. It is obvious that shear stress from bending was not enough to overcome the adhesive strength of ice and PVC (reported to be 234421 Pa (~34 psi) [22]). The fracture had introduced localised stress concentration which had contributed to the crack propagation at the interface and hence lead to the separation of ice from the PVC surface [29].

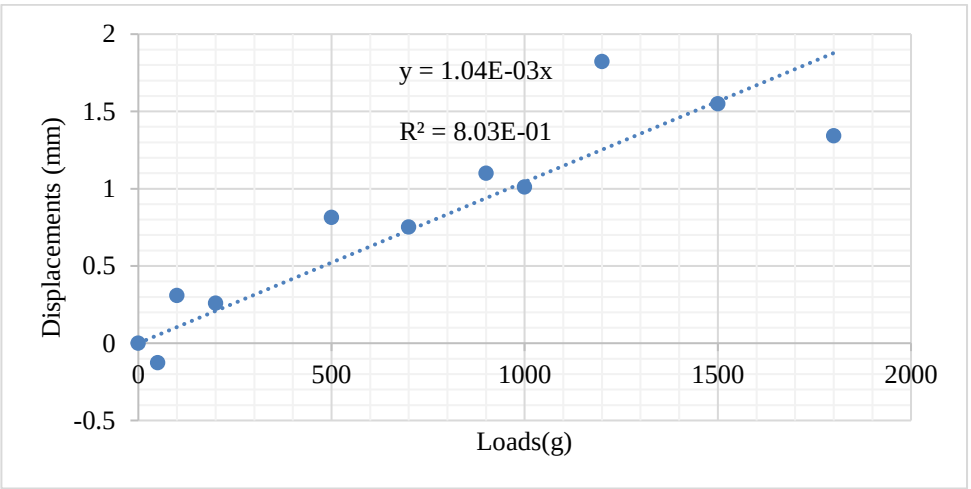

Figure 10: Displacement with variation in load for 3 mm thick ice sample

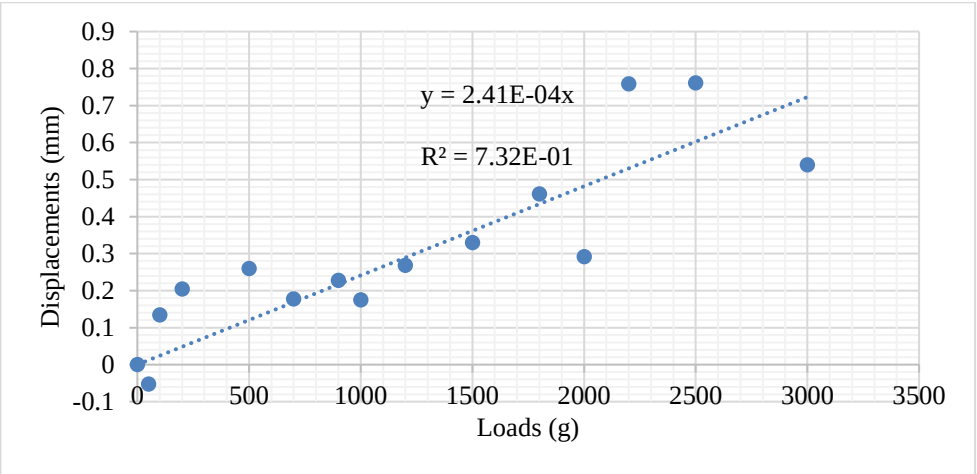

Figure 11: Displacement with variation in load for 5 mm thick ice sample

Table 4: Young's moduli of ice from the experimental results

Thickness of ice (mm)	Assumed PVC Young's Modulus (MPa)	Ice Young's Modulus from Experiments (GPa)	Deviation in results (GPa) based on R-squared value
3	1.5	4.70	+/- 0.93
	7	4.70	+/- 0.93
	15	4.70	+/- 0.93
5	1.5	3.85	+/- 1.03
	7	3.85	+/- 1.03
	15	3.85	+/- 1.03

Figure 12: Failure in 3 mm ice sample

Figure 13: Failure in a 5 mm ice sample

3.3 Numerical Simulations Results

Numerical analysis was carried out in ANSYS® Multiphysics. Results of maximum displacement in samples with load and longitudinal stresses are obtained. Figure 14 shows displacement results from a 5 mm sample under a loading of 3500g. Numerical results of displacement gradient with load are 1.036E-03 mm/g and 2.409E-04 mm/g for 3 mm sample and 5 mm sample respectively.

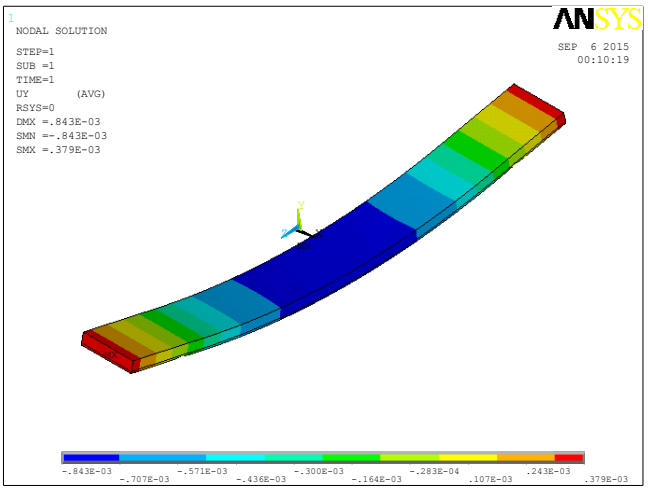

Figure 14: Displacement in the sample with 5 mm ice thickness loaded under 3500g.

The obtained longitudinal stress results for a 3 mm sample under a loading of 1800 g are shown in Figure 15 with a zoomed-in view shown in Figure 16.

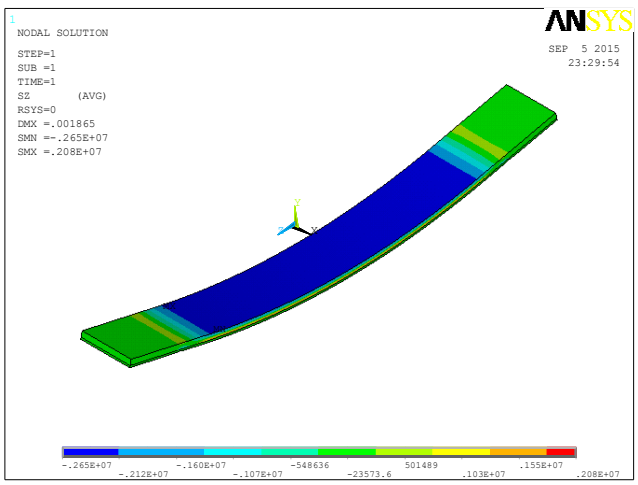

Figure 15: Longitudinal stress in the sample with 3 mm ice thickness loaded under 1800g.

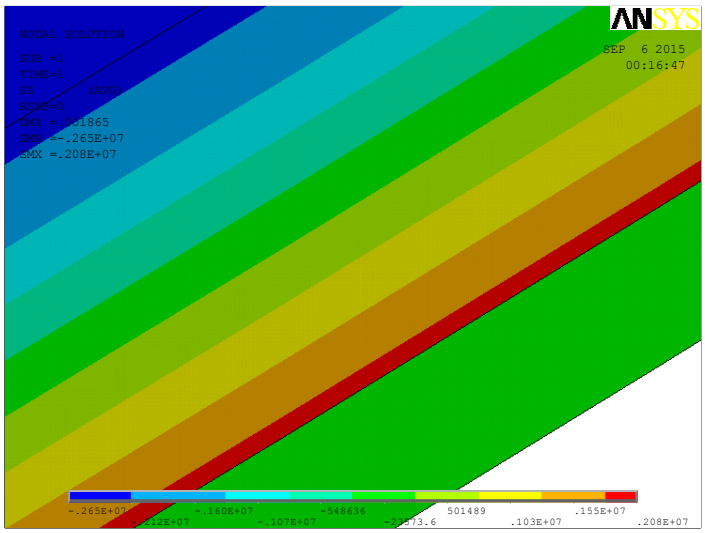

Figure 16: Zoomed-in view of longitudinal stress in the sample with 3 mm ice thickness loaded under 1800 g.

The obtained longitudinal stress results for a 5 mm sample under a loading of 3500 g are shown in Figure 17 with a zoomed-in view shown in Figure 18.

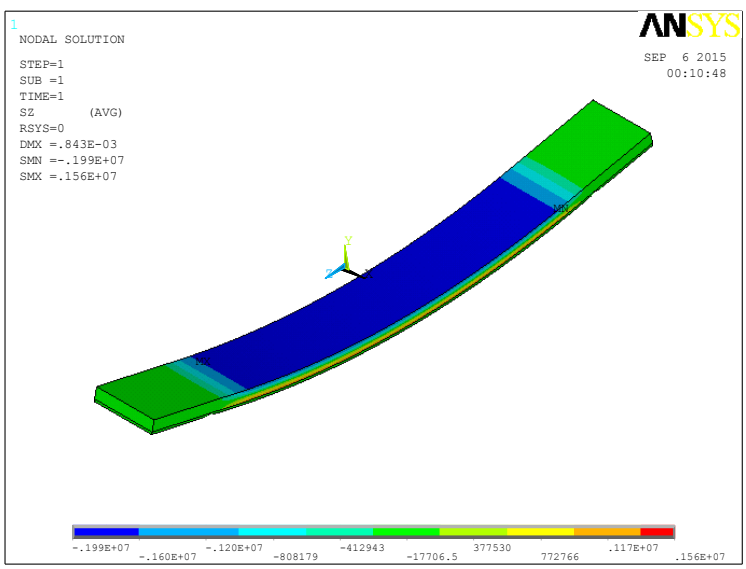

Figure 17: Longitudinal stress in the sample with 5 mm ice thickness loaded under 3500 g.

The maximum tensile longitudinal stresses experienced by the samples are 2.08 MPa and 1.56 MPa for 3mm and 5mm thickness of ice sample respectively.

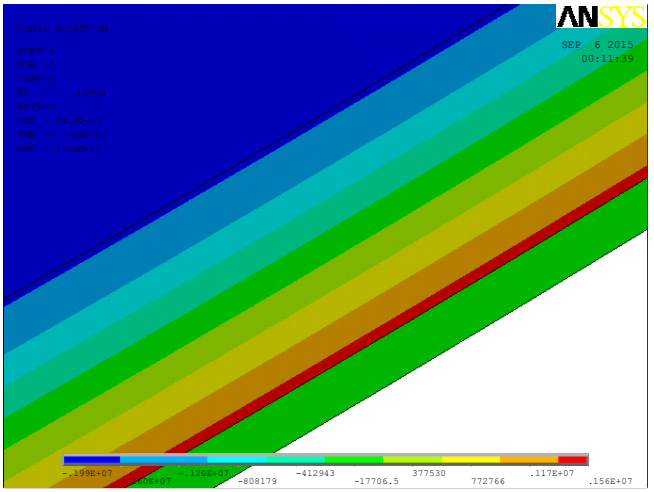

Figure 18: Zoomed-in view of longitudinal stress in the sample with 5 mm ice thickness loaded under 3500g.

3.4 Comparison of Theoretical, Experimental and Simulation Results

It can be noted that values of displacement with load gradient and longitudinal stresses are in good agreement within different methodologies. Displacement with load gradients for various samples tested using theoretical, experimental and numerical analysis are presented in Table 5. Longitudinal stresses obtained through theoretical, experimental and numerical analysis are given in Table 6.

Table 5: Comparison of displacement with load gradients (mm/g) (E_{ice} = 4 GPa and E_p = 15 MPa).

Ice thickness on 1 mm thick PVC sample	**Theoretical analysis using rule of mixture and beam theory**	**Experimental results**	**Numerical results using FEM (ANSYS® Multiphysics)**
3 mm	1.20E-03	1.04E-03	1.036E-03
5 mm	2.31E-04	2.41E-04	2.409E-04

Table 6: Comparison of longitudinal tensile stresses (MPa) (E_{ice} = 4 GPa and E_p = 15 MPa)

Ice thickness on 1 mm thick PVC sample	**Load at the time of failure (g)**	**Theoretical analysis using rule of mixture and beam theory**	**Experimental results**	**Numerical results using FEM (ANSYS® Multiphysics)**
3 mm	1800	1.96	1.96	2.08
5 mm	3500	1.37	1.37	1.56

There is acceptable variation between theoretical, experimental and numerical results. This can be associated with instrumental and numerical errors.

4. CONCLUSION

In this paper, ice adhesion over an arbitrary material of PVC has been investigated using theoretical analysis, experimental and numerical approaches. The theoretical study of this work is based on the use of the Euler-Bernoulli beam theory to solve a four-point bending problem to give the correlation of displacements with load, longitudinal stress and shear stress, and the rule of mixtures to derive common variables from two materials, such as Young's modulus, moment of inertia, and moment of area. Since adhesive forces can be categorized as either electrostatic, diffusion, mechanical and chemical as per the literature, there is no general correlation to work out the adhesive strength of ice over a particular surface except via experiments. Experiments with the help of theoretical analysis revealed the material properties of ice such as Young's modulus and tensile strength. The numerical analysis provided detailed results of displacement and longitudinal stresses in the two-material beam. A good agreement among theoretical, experimental and numerical results confirms that ice can separate from a surface even when the shear force is not enough to overcome the adhesive strength. From the results it can be concluded that during the test the shear force is not enough to overcome the adhesive strength. Nonetheless, as fracture happens, the ice separates from the surface, which is associated with the crack propagation theory.

ACKNOWLEDGEMENT

We would like to acknowledge the support of Dr. Guy Beeri Mauseth, Prof. Annette Meidell, Umair Mughal at the UiT The Arctic University of Norway and Dr. Matthew Carl Homola at Nordkraft AS, Narvik, Norway.

REFERENCES:

[1] Wahl, D. and P. Giguere, Ice Shedding and Ice Throw–Risk and Mitigation. General Electric Wind Application Engineering Group of GE Energy, 2006.
[2] Schulson, E.M., The structure and mechanical behavior of ice. JOM, 1999. 51(2): p. 21-27.
[3] Hobbs, P.V., Ice Physics. 2010: OUP Oxford.
[4] Fikke, S., et al., Cost 727: atmospheric icing on structures. Measurements and data collection on icing: State of the Art, Publication of MeteoSwiss, 2006. 75(110): p. 1422-1381.
[5] 12494, I., Atmospheric icing of structures. 2001.
[6] Voitkovskii, K., The mechanical properties of ice. 1962, DTIC Document.
[7] Nimmo, F. What is the Young's Modulus of Ice? in Workshop on Europa's Icy Shell: Past, Present, and Future. 2004.
[8] Gold, L.W., On the elasticity of ice plates. Canadian journal of civil engineering, 1988. 15(6): p. 1080-1084.
[9] Riahi, M.M., Numerical and Experimental Studies of the Mechanical Behaviour at the Ice / Aluminium Interface. 2007, University of Quebec, Canada.
[10] Barron, J., Investigators sift for clues to crash at La Guardia. New York times, 1992. 24.
[11] Ronsten, G., Svenska erfarenheter av vindkraft i kallt klimat nedisning, iskast och avisning. Elforsk rapport, 2004. 4: p. 13.
[12] Jasinski, W.J., et al., Wind turbine performance under icing conditions. Journal of Solar Energy Engineering, 1998. 120(1): p. 60-65.

[13] Jellinek, H.H.G., Adhesive properties of ice. Journal of colloid science, 1959. 14(3): p. 268-280.
[14] Kulinich, S. and M. Farzaneh, Ice adhesion on super-hydrophobic surfaces. Applied Surface Science, 2009. 255(18): p. 8153-8157.
[15] Landy, M. and A. Freiberger, Studies of ice adhesion: I. Adhesion of ice to plastics. Journal of colloid and interface science, 1967. 25(2): p. 231-244.
[16] Houwink, R. and G. Salomon, Adhesion and adhesives, Vol. 1. 1965, Elsevier, New York.
[17] Seidler, P., New theories of adhesion of high polymers. Adhaesion, 1963. 7: p. 503-512.
[18] Krotova, N., et al., Investigation of various types of adhesion bonds. 1965, DTIC Document.
[19] Voiutskii, S.S., Autohesion and adhesion of high polymers. 1963.
[20] Wake, W., Theories of adhesion and uses of adhesives: a review. Polymer, 1978. 19(3): p. 291-308.
[21] Adhesion Science and Engineering: Surfaces, Chemistry and Applications. 2002: Elsevier Science.
[22] Bikerman, J.J., The science of adhesive joints. 2013: Elsevier.
[23] Wilkes, C.E., et al., PVC Handbook. 2005: Hanser.
[24] Ramesh, S., T. Winie, and A.K. Arof, Investigation of mechanical properties of polyvinyl chloride–polyethylene oxide (PVC–PEO) based polymer electrolytes for lithium polymer cells. European Polymer Journal, 2007. 43(5): p. 1963-1968.
[25] Bauchau, O.A. and J.I. Craig, Structural Analysis: With Applications to Aerospace Structures. 2009: Springer Netherlands.
[26] Lu, T. and N. Fleck, The thermal shock resistance of solids. Acta Materialia, 1998. 46(13): p. 4755-4768.
[27] ANSYS®, Academic Research, Theory Reference, in Mechanical APDL Guide. release 14.0.
[28] Currier, J. and E. Schulson, The tensile strength of ice as a function of grain size. Acta Metallurgica, 1982. 30(8): p. 1511-1514.
[29] Sih, G.C., A special theory of crack propagation, in Mechanics of Fracture Initiation and Propagation. 1991, Springer Netherlands. p. 1-22.